Atmos. Chem. Phys. Discuss., 7, 8571–8595, 2007
www.atmos-chem-phys-discuss.net/7/8571/2007/

Atmospheric Chemistry and Physics Discussions

The Coupled Aerosol and Tracer Transport model to the Brazilian developments on the Regional Atmospheric Modeling System (CATT-BRAMS) – Part 2: Model sensitivity to the biomass burning inventories

K. M. Longo[1], S. R. Freitas[1], A. Setzer[1], E. Prins[2], P. Artaxo[3], and M. O. Andreae[4]

[1]Center for Weather Forecasting and Climate Studies, INPE, Cachoeira Paulista, Brazil
[2]UW-Madison Cooperative Institute for Meteorological Satellite Studies, Madison, WI, USA
[3]Institute of Physics, University of São Paulo, Brazil
[4]Max Planck Institute for Chemistry, Mainz, Germany

Received: 20 April 2007 – Accepted: 5 June 2007 – Published: 20 June 2007

Correspondence to: K. M. Longo (longo@cptec.inpe.br)

Abstract

We describe an estimation technique for biomass burning emissions in South America based on a combination of remote sensing fire products and field observations. For each fire pixel detected by remote sensing, the mass of the emitted tracer is calculated based on field observations of fire properties related to the type of vegetation burning. The burnt area is estimated from the instantaneous fire size retrieved by remote sensing, when available, or from statistical properties of the burn scars. The sources are then spatially and temporally distributed and assimilated daily by the Coupled Aerosol and Tracer Transport model to the Brazilian developments on the Regional Atmospheric Modeling System (CATT-BRAMS) in order to perform the prognostic of related tracer concentrations. Two other biomass burning inventories are simultaneously used to compare the emission strength in terms of the resultant tracer distribution. Several evaluations of the model with the three emission estimations were performed, comparing results with direct measurements of carbon monoxide both near-surface and airborne, as well as remote sensing derived products. Model results with the methodology of estimation introduced in this paper show a relatively good agreement with the direct measurements and MOPITT data product; pointing out the reliability of the model from local to regional scales.

1 Introduction

The high concentration of aerosol particles and trace gases observed in the Amazon and Central Brazilian atmosphere during the dry season is associated with intense anthropogenic biomass burning activity (vegetation fires). A widely cited estimate suggests that biomass burning in South America is responsible for the emission of 30 Tg year^{-1} of aerosol particles to the atmosphere (Andreae, 1991). Most of the particles are in the fine particle fraction of the size distribution, which can remain in the atmosphere for approximately a week (Kaufman, 1995). In addition to aerosol particles,

biomass burning produces water vapor and carbon dioxide, and is a major source of other compounds such as carbon monoxide (CO), volatile organic compounds, nitrogen oxides and organic halogen compounds (Andreae and Merlet, 2001). In the presence of abundant solar radiation and high concentrations of NO_x, the oxidation of CO and hydrocarbons results in ozone (O_3) formation. Undoubtedly, biomass burning emissions have a strong impact on the tropospheric and stratospheric chemical composition and are an important agent of weather and climate change. Therefore, the estimation of the amounts injected into the atmosphere at regional as well as global scales is needed.

The most common way to estimate emissions from vegetation fires, the so-called "bottom-up" approach, is through an initial estimation of the quantity of biomass consumed through combustion. This estimation can be accomplished if information on the aboveground biomass density, the combustion factor (the fraction of the fuel load actually combusted) and the area burned is available. Following this method, the amount of specific chemical species can be obtained by using the associated emission factor (fraction of mass of compound emitted per mass of fuel burned, on a dry mass basis). A thorough review of emission factors was presented by Andreae and Merlet (2001). Several authors have been working on estimates of biomass consumption by combustion. Hao and Liu (1994) built a database for the spatial (5 degrees) and temporal (monthly) distribution of the amount of biomass burned in tropical America, Africa, and Asia during the late 1970s. More recently, Giglio et al. (2006) and van der Werf et al. (2006), using burned area estimate from remote sensing, a biogeochemical model and emission factors from literature, estimated fire emissions during the 8-year period from 1997 to 2004. This dataset, called Global Fire Emissions Database (GFEDv2), has 1×1 degree spatial resolution with 8-day and one-month time steps. Duncan et al. (2003) combined fire-count data from the Along Track Scanning Radiometer (ATSR) and the Advanced Very High Resolution Radiometer (AVHRR) World Fire Atlases to determine the typical seasonal and interannual variability of biomass burning emissions. Using the total Ozone Mapping Spectrometer (TOMS) Aerosol Index as a proxy

to estimate the strength of emissions, the authors estimated the mean variability of CO emissions from biomass burning. Recent and promising methodologies use the fire radiative energy to estimate the emission rates (Kaufman et al., 2003, Riggan et al., 2004, Ichoku and Kaufman, 2005).

In this paper we describe and evaluate an estimation technique for biomass burning emissions based on a combination of remote sensing fire products and field observations. The developed inventory is then applied to simulate the 2002 dry season pyrogenic CO over South America (SA), when and where the field campaigns LBA Smoke, Aerosols, Clouds, Rainfall, and Climate (SMOCC) and Radiation, Cloud, and Climate Interactions in the Amazon during the dry-to-wet Transition Season (RaCCI) took place. The paper is organized as follows: in Sect. 2, the technique is described. Model configuration and a general discussion about its performance for 2002 dry season simulation are introduced in Sect. 3. Section 4 explores model results and comparisons with available observed data from the meteorological point of view. Model results for CO are evaluated using surface measurements, airborne and remote sensing retrieved data in Sect. 5. Our conclusions are discussed in section 6.

2 The biomass burning emissions inventory

The biomass burning emission parameterization aspect of this paper is based on Freitas et al. (2005) with several improvements. Basically, for each fire pixel detected, the mass of the emitted tracer is calculated by the following expression, which takes into consideration the estimated values for the amount of above-ground biomass available for burning (α), the combustion factor (β) and the emission factor (EF) for a certain specie [η], taking into account the type of vegetation, and the burning area (a_{fire}) for each burning event.

$$M^{[\eta]} = \alpha_{\text{veg}} \cdot \beta_{\text{veg}} \cdot EF^{[\eta]}_{\text{veg}} \cdot a_{\text{fire}}, \quad (1)$$

A hybrid remote sensing fire product is used to minimize missing remote sensing observations. The fire database actually utilized is a combination of the Geostationary Operational Environmental Satellite - Wildfire Automated Biomass Burning Algorithm (GOES WF_ABBA product (http://cimss.ssec.wisc.edu/goes/burn/wfabba.html; Prins et al., 1998), the Brazilian National Institute for Space Research fire product, which is based on the Advanced Very High Resolution Radiometer (AVHRR), aboard the NOAA polar orbiting satellites series (http://www.cptec.inpe.br/queimadas; Setzer and Pereira, 1987) and the Moderate Resolution Imaging Spectroradiometer (MODIS) fire product (http://modis-fire.umd.edu; Giglio et al., 2003). The three fire products databases are combined using a filter algorithm to avoid double count of the same fire, by eliminating additional fires within a circle of 1 km radius. The fire detection maps are merged with 1 km resolution land use (Belward, 1996) and carbon in live vegetation datasets (Olson et al., 2000 and Houghton et al., 2001) to provide the associated emission factor, combustion factor and carbon density. The emission and combustion factors for each biome are based on the work of Ward et al. (1992) and Andreae and Merlet (2001). The burnt area is estimated by the instantaneous fire size retrieved by remote sensing, when available, or by statistical properties of the scars. Fires detected according the GOES WF_ABBA product have the burnt area estimated by the instantaneous fire size for each non-saturated and non-cloudy fire pixel, where it is possible to retrieve sub-pixel fire characteristics. For GOES WF_ABBA detected fires that have no information about the instantaneous fire size, a mean instantaneous fire size of 0.14 km^2 (calculated from the GOES ABBA database of the previous years) is used. For fires processed by the MODIS system, a mean value of 0.22 km^2 of burnt area is applied according to J. M. C. Pereira (personal communication, 2007). The AVHRR fires also use the same value as for MODIS for the estimated burnt area. The total emission per species for each model grid box, taking into account all the possible

observed sub-grid fires burning different types of vegetation, is then given by:

$$Q^{[\eta]} = \frac{r(t)}{\rho_0 \Delta V} \sum_{\substack{\text{fires\_} \in \\ \text{Grid\_Box}}} M^{[\eta]}, \quad (2)$$

where ρ_0 is the basic state air density, $\Delta \boldsymbol{V}$ is the volume of the first physical grid cell and the Gaussian function ***r(t)***, centered at 17:45 UTC, modulates the emission diurnal cycle, following the study of Prins et al. (1996) about fire diurnal variability over SA. Then, using this methodology, the emission sources are distributed with the same spatial and temporal resolution as that of the atmospheric transport model, and assimilated daily according to the biomass burning spots actually observed by the satellites. Figure 1 summarizes all the sources of information used to estimate biomass burning emissions according to this technique, which we named Brazilian Biomass Burning Emission Model (3BEM). In addition to the biomass burning emissions, we included the biofuel use and agricultural waste burning inventory developed by Yevich and Logan (2003).

In this study, two other biomass burning emission inventories, built with different approaches and spatial resolution are considered: the EDGAR database (Olivier et al., 1996; Olivier et al., 1999) and that of Duncan et al. (2003, hereafter D2003). These two inventories are shown together with 3BEM in Fig. 2 and Fig. 3, in terms of the spatial and temporal distribution of CO emissions over SA for the months of August to November 2002. In Fig. 2, the first column from the left corresponds to the estimation obtained by the 3BEM model with 35 km resolution; the second column refers to D2003 mean seasonal estimation with 1 degree resolution; and in the last column appears the EDGAR with 2.5 degrees resolution. 3BEM shows general agreement with the D2003 estimation for August and September in the deforestation areas. However, in the cerrado (savanna) areas, D2003 emissions are several times higher than 3BEM, in general. For October and November, the inventories show larger differences. Also both estimations obviously have finer scales in comparison with EDGAR, which prescribes

a too wide and smooth emission field.

This comparison highlights the additional features of 3BEM relative to the other two inventories: a spatial resolution that can be as fine as the pixel size of the satellite sensor used for the fire detection, a temporal resolution of a day or less, and also the fact that the emission is placed only in regions where fires were in fact observed. We shall next explore the sensitivity of the atmospheric transport model to the inclusion of this level of detail in the inventory.

3 Model CO results and evaluation using 2002 dry season data

The three inventories described above were introduced into the CATT-BRAMS model system (Freitas et al., 2007). Simulations for the 2002 dry season were performed to compare model results using the three inventories described with observed and remote sensing derived data.

The model configuration had 2 grids: the coarse grid with 140 km horizontal resolution covering the South American and African continents, its main purpose being to simulate the intermittent smoke inflow from the African fires to South America and to coordinate with and compare to the long-range transport of smoke from fires in South America to the Atlantic Ocean; and the nested finer grid with a horizontal resolution of 35 km, covering only SA. The vertical resolution for both grids varies telescopically with higher resolution at the surface (150 m), increasing stepwise with a ratio of 1.07 up to a maximum vertical resolution of 850 m at the top of the model at 23 km (a total of 42 vertical levels). The simulation started on 00:00 UTC 15 July 2002 and the results for August, September and October are discussed. More details about the model configuration can be found in Freitas et al. (2007). Four tracers were simulated representing CO emitted according to each inventory with the same initial values. The general mass

continuity equation for tracers solved in the CATT-BRAMS model is

$$\frac{\partial \bar{s}}{\partial t} = \underbrace{\left(\frac{\partial \bar{s}}{\partial t}\right)_{\text{adv}}}_{\text{I}} + \underbrace{\left(\frac{\partial \bar{s}}{\partial t}\right)_{\substack{\text{PBL}\\ \text{diff}}}}_{\text{II}} + \underbrace{\left(\frac{\partial \bar{s}}{\partial t}\right)_{\substack{\text{deep}\\ \text{conv}}}}_{\text{III}} + \underbrace{\left(\frac{\partial \bar{s}}{\partial t}\right)_{\substack{\text{shallow}\\ \text{conv}}}}_{\text{IV}} + \underbrace{R}_{\text{V}} + \underbrace{Q}_{\text{VI}} , \qquad (3)$$

where $\bar{s}$is the grid box mean tracer mixing ratio, I represents the 3-D resolved transport term (advection by the mean wind), II is the sub-grid scale diffusion in the PBL, III and IV are the sub-grid transport by deep and shallow convection, term (V) is a generic sink term and refers to the dry deposition as well as chemical transformation of CO, and, finally, term (VI) is the source term which may or may not include the plume rise mechanism. The loss of CO by chemical transformation is included through a linearized removal with a lifetime of 30 days (Seinfeld and Pandis, 1998). Since the lifetime of CO is long, from 50 to occasionally a minimum of 15 days (Mauzerall et al., 1998), CO acts essentially as a passive tracer in the simulation. The CO in the simulations tends to flow out of the model, especially above the boundary layer, and boundary conditions control the concentration more than the linearized chemical removal (see Freitas et al., 2007 for more details). In this case the simulation was carried out with four CO tracers according to the following specifications. Three tracers named COE, COD and CODPSH did not include the plume rise mechanism, with the total CO mass (term VI) released into the model layer closest to the surface. The transport processes for these three tracers included the terms I, II, III and IV, and the source emission inventories used were EDGAR, D2003 and 3BEM, respectively. A fourth tracer (named COALL), beyond the terms I, II, III and IV, included the plume rise mechanism through a 1-D plume model (Freitas et al., 2006) and also used 3BEM inventory. In the last case, the smoldering fraction of the total emission was released in the first model layer and the flaming fraction released at the effective injection height provided by the plume rise model. The simulation with the CODPSH tracer, using 3BEM, but without the plume rise, was performed in order to provide a consistent comparison with EDGAR and D2003 prescriptions.

In the next sub-sections we will compare these model results with observations at three different scales: local – near surface level measurements; regional - airborne vertical profiles; and large scale – remote sensing data. The discussion to follow is based on the CATT-BRAMS model results with the three different emission estimates on the regional grid domain covering SA with 35 km resolution.

3.1 Model comparison with SMOCC/RaCCI 2002 surface and airborne measurements

In the framework of the SMOCC/RaCCI campaign, from 10 September to early November 2002, measurements of CO near surface level were performed at the Ouro Preto do Oeste pasture site, in Rondônia, Brazil (Andreae et al., 2004). Figure 4 shows the CO time series, comparing observations and the model results with the three different emission estimates: 3BEM, EDGAR and D2003. This comparison between the near-surface daily average measurements and model results clearly indicates a better skill of the 3BEM inventory relatively to the others.

The model CO using the 3BEM technique and without the plume rise mechanism (CODPSH) presents much more consistent time variability and range of values with the near-surface measurements. Though we noticed that the CO-3BEM do not follow very close the observations during periods when the atmosphere is very polluted, such as the period from 19 to 22 September, this underestimation might be related with fire misdetection below the thick smoke column. Even so, using monthly time resolution inventories like EDGAR and D2003, the model could not capture the observed time variability of the near surface CO concentration. Also is evident that the strength of emissions of EDGAR and D2003 for October is too weak, at least for the 2002 dry season and EDGAR also performed badly for September in terms of the emission intensity.

This discussion is also anchored by the linear regression of observed CO versus modeled values (in the detail of the Fig. 4) with correlation coefficients (R^2) of approximately 0.66, 0.37 and 0.03 for 3BEM, EDGAR and D2003, respectively. The large

standard deviation of the mean of the observed CO (shown by the error bars) and the strong time daily variability are due the proximity of the measurement site to many fire spots. While the emission inventories based on climatologic information are not able to capture this variability and the intensity, the 3BEM methodology closely follows the observations, both in terms of intensity and day-to-day variability. As the three tracers were simulated using exactly the same dynamics, the results of this section point out the requirement for accurate information regarding timing and location of fires in the emissions inventories in order to simulate realistically the time variability of near-surface associated air pollution.

In order to evaluate the model results when describing the vertical structure of the smoke haze layer and to examine its sensitivity to the choice of emission fields, we performed a comparison of the simulated CO profiles in the PBL and lower troposphere with observed data using SMOCC/RaCCI campaign airborne measurements (Andreae et al., 2004, Freitas et al., 2007). The typical maximum altitude reached by the SMOCC/RaCCI aircraft was 5 km. Figure 5 shows the vertical profiles for model results and observations for sixteen flights. The mean and standard deviations (STD) of the observed CO profiles are shown; note that STD represents the actual variability of the concentrations in the vertical layer, not the measurement error. The EDGAR and D2003 model results show a PBL typically much cleaner than observations, with the model results for CO concentration ranging from 150 to 300 ppb. D2003 presents the worst performance in spite of its better horizontal resolution and estimation approach when compared to EDGAR. In contrast, the 3BEM model results present more variability on a day-to-day basis, with values ranging from 150 to 900 ppb, following more closely the observed pattern. Typically, the large STDs are due to aircraft passages through isolated smoke plumes, and even for those cases the 3BEM model results usually represent the mean values very well. As expected, the 3BEM model with the plume-rise mechanism included results in a less polluted PBL, and very often the 3BEM model results with plume-rise show a better agreement with observations compared to simulations where this effect is disregarded, such as for the flights SMOCC 18, 21, 27

and 28. Nevertheless, it is clear that the model results are much more sensitive to the emission choice than to the inclusion of the plume-rise mechanism. This point is reinforced by a composite vertical profile where all the available profiles are plotted together (Fig. 6). Even though previous work has shown the importance of including the plume-rise mechanism (Freitas et al., 2006) this must be based on a correct estimation of the total emission.

3.2 Model comparisons with MOPITT CO data

The model performance on larger scales and including mid- to upper tropospheric levels is evaluated in this section using data retrieved by the "Measurements of Pollution in the Troposphere" (MOPITT) instrument, onboard the Earth Observing System Terra satellite. MOPITT retrievals of tropospheric CO mixing ratio (ppb) are reported for 3 pressure levels: 700, 500 and 250 hPa (Deeter et al., 2003). Because MOPITT data have large horizontal areas without valid data due to swath width and cloud cover, the model results, after applying the averaging kernel and a priori profile, and using retrievals with <50% a priori contribution, and MOPITT data were monthly averaged. Figure 7 and Fig. 8 shows the comparisons at the large scale grid for the months of August and October, respectively. The model results for 3BEM are in the first column from the left; the second column refers to EDGAR; and in the last column appear the results for the D2003emissions. The quantity depicted in the above mentioned figures is the relative model error (ME) defined as

$$\mathrm{ME}=100 \times \frac{\mathrm{CO}_{\mathrm{mopitt}}-\mathrm{CO}_{\mathrm{model}}}{\mathrm{CO}_{\mathrm{mopitt}}} \quad (4)$$

where $\mathrm{CO}_{\mathrm{model}}$ is the monthly mean of the model CO mixing ratio after applying the averaging kernel and a priori fraction <50%. According to the above definition, positive values mean that model results are underestimated in reference to the MOPITT retrieved data and vice-versa. The model error for CODPSH using 3BEM is shown in the

left column (letters A, B and C), for COE using EDGAR appears in the center (letters D, E and F) and, finally, COD model errors are on the right side (letters G, H and I).

For August (Fig. 7), 3BEM model errors are smaller at all levels while EDGAR and D2003 present similar numbers. All model results present similar errors at south of 30 S that might be associated to the lateral boundary condition, since this region is not usually affected by the biomass burning emissions. The regions where 3BEM have larger model errors are smaller in terms of area coverage than that one of the EDGAR and D2003, this characteristic is due to the large scale spatial emission of these inventories.

Over SA during August, the model error for the 250 and 500 hPa levels was below typically 10%, with few areas of 20% over the Amazon for 3BEM, while for the other two inventories it ranged from 20% to 35% with a few areas reaching 50%. For the 700 hPa level, the 3BEM also presents better skill over SA compared to EDGAR and D2003, with the 3BEM model error typically below 20%, against 35–50% for the others. In addition, we should keep in mind the lower reliability of MOPITT retrievals at low levels, due to the typically stronger influence of the assumed a priori for retrieved surface level CO concentration than for higher levels (Deeter et al., 2003). For October (Fig. 8), although 3BEM model errors were greater than for August, 3BEM still showed better skill than EDGAR and D2003.

4 Discussion and conclusions

A biomass burning emission technique developed for South America, here named 3BEM, has been described and evaluated via performance analysis of the atmospheric transport model CATT-BRAMS against observations. The results using 3BEM were compared to those obtained using two other biomass burning emissions inventories, EDGAR and D2003. 3BEM features include a fine spatial resolution, adjustable to the resolution of the atmospheric transport model, and a temporal resolution that includes realistic daily and even diurnal cycling. The two other biomass burning inventories

evaluated, EDGAR and D2003, are fundamentally climatological with 2.5 and 1.0 degree spatial resolution, respectively, and monthly temporal resolution. The goals of this study include evaluation of the benefits of including this fine level of detail at the various scales of interest, as well as validation of the 3BEM emission inventories.

For the local and regional scales, our results clearly indicate the need for the inclusion of diurnal and daily variability as well as higher spatial resolution. For the large scale, while for climatological studies there is no need for a higher temporal resolution, for investigations of isolated and particularly intense long range transport events the daily variability is also a requirement.

In general, the performance of the CATT-BRAMS model fed with 3BEM against observations is undoubtedly superior to results obtained with the other two inventories. This was true for all scales of evaluation: local, regional and large-scale. Although the 3BEM inventory is based on a very simple approach and relies on input parameters with well-known inaccuracies, it is actually capable to provide valid estimates of the biomass burning emission fields, as long as appropriate input parameters are chosen. An approach similar to 3BEM has also been used by others groups with good results (Wang et al., 2006).

The promising agreement between model results and local observations and remote-sensing-derived data of CO at several scales (local to large-scale) shown in this paper as well as by Freitas et al. (2007, including also particulate matter, PM2.5) indicate that 3BEM is a valid approach for South America. However, the extension of this kind of approach to other regions requires the availability of detailed datasets described before, as well as fire count information in terms of location, timing, diurnal cycle and estimated fire size and/or burnt area. Comparisons with the recent released version of GFEDv2 (8-day time resolution) will appear in a forthcoming paper, where we will focus mainly on whether the 8-day time resolution is enough to capture the time variability of near-surface observations of CO and PM2.5 during the SMOCC/RaCCI field campaign, as well as the strength of emissions.

Acknowledgements. We thank all members of the LBA-SMOCC/RACCI Science Teams for their support during the field campaign, especially J. von Jouanne, M. Welling, P. Guyon, G. Nishioka, T. Germano, and the pilots of the INPE aircraft. We acknowledge partial support of this work by NASA Headquarters (NRA-03-OES-02 and NRA-02-OES-06) and CNPq (305059/2005-0). This work was carried out within the framework of the project "Monitoramento de emissões de queimadas e avaliação das observações de qualidade do ar em Três Lagoas – MS" in collaboration with CENPES/Petrobras; the LBA Smoke, Aerosols, Clouds, Rainfall, and Climate (SMOCC) project (funded by the Environmental and Climate Program of the European Commission under contract N° EVK2-CT-2001-00110-SMOCC and by the Max Planck Society), and Radiation, Cloud, and Climate Interactions in the Amazon during the DRY-TO-WET Transition Season (RACCI) project (funded by FAPESP and Instituto do Milenio/LBA/CNPq/MCT).

References

Andreae, M.: Biomass burning: its history, use and distribution and its impact on environmental quality and global climate, in: Global Biomass Burning: Atmospheric, Climatic and Biospheric Implications, edited by: J. S. Levine, pp. 3–21, MIT Press, Cambridge, Mass, 1991.

Andreae, M. and Merlet, P.: Emission of trace gases and aerosols from biomass burning, Global Biogeochem. Cycles, 15, 4, 955–966, 2001.

Andreae, M., Rosenfeld, D., Artaxo, P., Costa, A., Frank, G., Longo, K. M., and Silva Dias, M A. F.: Smoking rain clouds over the Amazon, Science, 303, 1342–1345, 2004.

Belward, A.: The IGBP-DIS global 1 km land cover data set (DISCover)-proposal and implementation plans, IGBP-DIS Working Paper No.13, Toulouse, France, 1996.

Deeter, M. N., Emmons, L. K., Francis, G. L., Edwards, D. P., Gille, J. C., Warner, J. X., Khattatov, B., Ziskin, D., Lamarque, J.-F., Ho, S.-P., Yudin, V., Attié, J.-L., Packman, D., Chen, J., Mao, D., and Drummond, J. R.: Operational carbon monoxide retrieval algorithm and selected results for the MOPITT instrument, J. Geophys. Res., 108(D14), 4399, doi:10.1029/2002JD003186, 2003.

Duncan, B., Martin, R., Staudt, A., Yevich, R., and Logan, J.: Interannual and seasonal variability of biomass burning emissions constrained by satellite observations, J. Geophys. Res., 108(D2), 4100, doi:10.1029/2002JD002378, 2003.

Giglio, L., Descloitres, J., Justice, C. O., and Kaufman, Y. J.: An enhanced contextual fire detection algorithm for MODIS, Remote Sensing of Environment, 87, 273–282, 2003.

Giglio, L., van der Werf, G. R., Randerson, J. T, Collatz, G. J., and Kasibhatla, P. S.: Global Estimation of Burned Area using MODIS Active Fire Observations, Atmos. Chem. Phys., 6, 957–974, 2006, http://www.atmos-chem-phys.net/6/957/2006/.

Ichoku, C. and Kaufman, Y. J.: A method to derive smoke emission rates from MODIS fire radiative energy measurements. IEEE Transactions on Geoscience and Remote Sensing, 43, 11, 2636–2649, 2005.

Houghton, R. A., Lawrence, K. T., Hackler, J. L., and Brown, S.: The spatial distribution of forest biomass in the Brazilian Amazon: a comparison of estimates, Global Change Biol., 7(7), 731–746, 2001.

Kaufman, Y.: Remote sensing of direct and indirect aerosol forcing, in: Aerosol Forcing of Climate, edited by: Charlson, R. J. and Heintzenberg, J., 297-332, John Wiley & Sons Ltd, Chichester, 1995.

Kaufman, Y. J., Ichoku, C., Giglio, L., Korontzi, S., Chu, D. A., Hao, W. M., Li, R. -R., and Justice, C. O.: Fire and smoke observed from the Earth Observing System MODIS instrument–products, validation, and operational use, Int. J. Remote Sensing, 24(8), 1765–1781, 2003.

Freitas, S. R., Longo, K. M., Silva Dias, M., Silva Dias, P., Chatfield, R., Prins, E., Artaxo, P., Grell, G., and Recuero, F.: Monitoring the transport of biomass burning emissions in South America, Environmental Fluid Mechanics, doi:10.1007/s10652-005-0243-7, 5(1–2), 135–167, 2005.

Freitas, S. R., Longo, K. M., Chatfield, R., Latham, D., Silva Dias, M. A. F., Andreae, M. O., Prins, E., Santos, J. C., Gielow R., and Carvalho Jr., J. A.: Including the sub-grid scale plume rise of vegetation fires in low resolution atmospheric transport models, Atmos. Chem. Phys. Discuss., 6, 11 521–11 559, 2006.

Freitas, S. R., Longo, K. M., Silva Dias, M., Chatfield, R., Silva Dias, P., Artaxo, P., Andreae, M. O., Grell, G., Rodrigues, L. F., Fazenda, A., and Panetta, J.: The Coupled Aerosol and Tracer Transport model to the Brazilian developments on the Regional Atmospheric Modeling System. Part 1: Model description and evaluation, Atmos Chem. Phys. Disccus., 7, 8525–8569, 2007.

Hao, W. M. and Liu, M.-H.: Spatial and temporal distribution of tropical biomass burning, Global Biogeochem. Cycles, 8(4), 495504, 1994.

Mauzerall, D., Logan, J., Jacob, D., Anderson, B., Blake, D., Bradshaw, J., Heikes, B., Sachse, G., Singh, H., and Talbot, B.: Photochemistry in biomass burning plumes and implications for tropospheric ozone over the tropical South Atlantic, J. Geophys. Res. 103(D7), 8401–8423, 1998.

Olson, J. S., Watts, J. A., and Allison, L. J.: Major World Ecosystem Complexes Ranked by Carbon in Live Vegetation: A Database (Revised November 2000). NDP-017. Available online [http://cdiac.esd.ornl.gov/ndps/ndp017.html] from Carbon Dioxide Information Analysis Center, Oak Ridge National Laboratory, Oak Ridge, Tennessee, USA, 2000.

Olivier, J., Bouwman, A., van der Maas, C., Berdowski, J., Veldt, C., Bloos, J., Visschedijk, A., Zandveld, P., and Haverlag, J.: Description of EDGAR Version 2.0: A Set of Global Emission Inventories of Greenhouse Gases and Ozone-Depleting Substances for All Anthr pogenic and Most Natural Sources on a per Country Basis and on a 1x1 Degree Grid, RIVM Report 771060 002/TNO-MEP Report R96/119, National Institute of Public Health and the Environment, Bilthoven, the Netherlands, 1996.

Olivier, J., Bouwman, A., Berdowski, J., Veldt, C., Bloos, J., Visschedijk, A., van der Maas, C., and Zandveld, P.: Sectoral emission inventories of greenhouse gases for 1990 on a per country basis as well as on 1x1 degree, Environ. Sci. Policy, 2, 241–264, 1999.

Prins, E., Feltz, J., Menzel, W., and Ward, D.: An overview of GOES-8 diurnal fire and smoke results for SCAR-B and 1995 fire season in South America, J. Geophys. Res., 103(D24), 31 821–31 835, 1998.

Riggan, P., Tissell, R., Lockwood, R., Brass, J., Pereira, J., Miranda, H., Miranda, A., Campos, T., and Higgins, R.: Remote measurement of energy and carbon flux from wildfires in Brazil, Ecol. Appl., 14, 3, 855–872, 2004.

Seinfeld, J. and Pandis, S.: Atmospheric Chemistry and Physics, John Wiley & Sons Inc., New York, 1998.

Setzer, A. and Pereira, M.: Amazonia biomass burnings in 1987 and an estimate of their tropospheric emissions, Ambio, 20, 19–22, 1991.

Van der Werf, G. R., Randerson, J. T., Giglio, L., Collatz, G. J., and Kasibhatla, P. S.: Interannual variability in global biomass burning emission from 1997 to 2004, Atmos. Chem. Phys., 6, 3423–3441, 2006, http://www.atmos-chem-phys.net/6/3423/2006/.

Yevich, R. and Logan, J.: An assessment of biofuel use and burning of agricultural waste in the developing world, Global Biogeochem. Cycles, 17(4), 1095, doi:10.1029/2002GB001952,

2003.
Wang J., Christopher, S., Nair, U., Reid, J., Prins, E., Szykman, J., and Hand, J.: Mesoscale modeling of Central American smoke transport to the United States: 1. "Top-down" assessment of emission strength and diurnal variation impacts, J. Geophys. Res., 111, D05S17, doi:10.1029/2005JD006416, 2006.
Ward, E., Susott, R., Kaufman, J., Babbit, R., Cummings, D., Dias, B., Holben, B., Kaufman, Y., Rasmussen, R., and Setzer, A.: Smoke and fire characteristics for cerrado and deforestation burns in Brazil: BASE-B Experiment, J. Geophys. Res., 97(D13), 14 601–14 619, 1992.

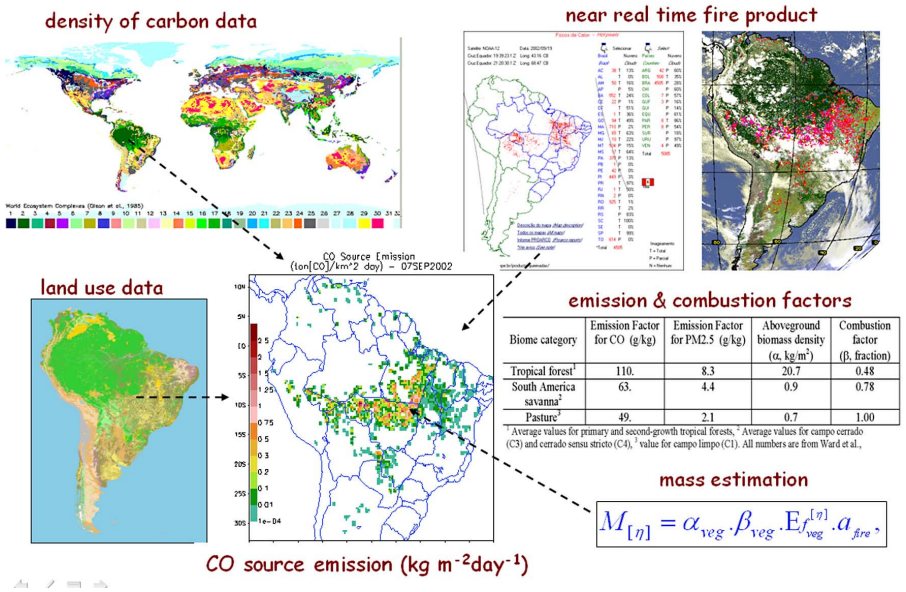

Biome category	Emission Factor for CO (g/kg)	Emission Factor for PM2.5 (g/kg)	Aboveground biomass density (α, kg/m²)	Combustion factor (β, fraction)
Tropical forest[1]	110.	8.3	20.7	0.48
South America savanna[2]	63.	4.4	0.9	0.78
Pasture[3]	49.	2.1	0.7	1.00

[1] Average values for primary and second-growth tropical forests, [2] Average values for campo cerrado (C3) and cerrado sensu stricto (C4), [3] value for campo limpo (C1). All numbers are from Ward et al.,

Fig. 1. Cartoon describing all sources of information used to estimate biomass burning emissions according to the 3BEM methodology.

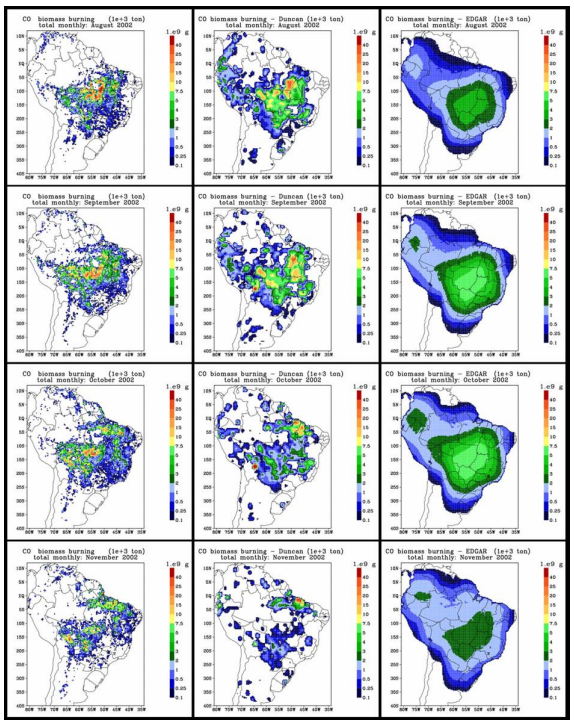

Fig. 2. The three biomass burning inventories: the first column from the left shows the spatial distribution of the CO emission estimation (10^{+3} ton) obtained for the months August to November 2002 with the technique described in this paper (3BEM), the second column refers to the D2003 estimation and the last column is the EDGAR product.

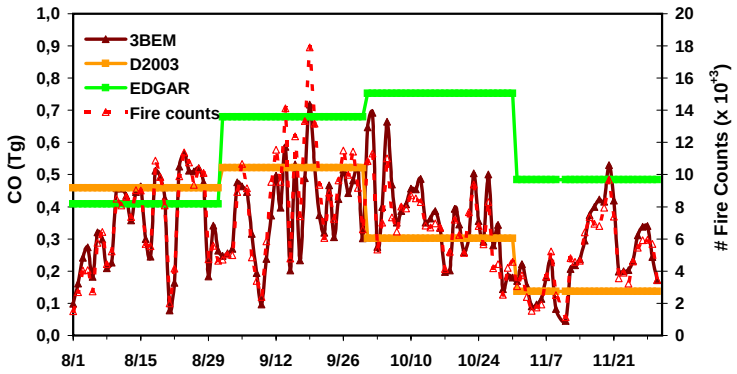

Fig. 3. The three biomass burning inventories: time series for the total pyrogenic CO emission estimate from SA (Tg) from 1 August to 30 November 2002 with 3BEM (dark red), EDGAR (green) and D2003 (orange), and the number of fire counts (red).

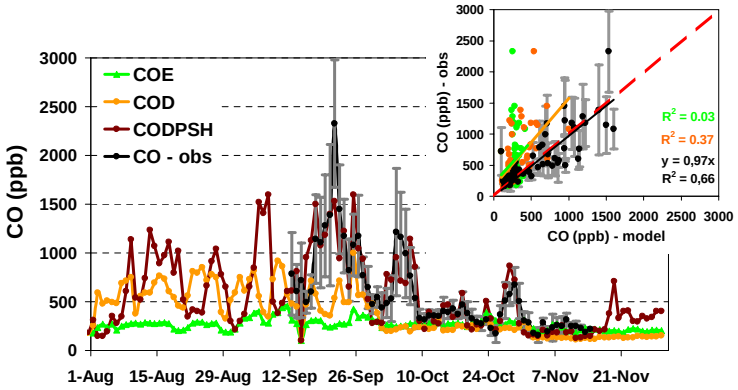

Fig. 4. Time series and scatter plot with linear regression (in the detail) with comparison between near surface CO (ppb), observed (black) and model results with the 3BEM emission inventory (dark red), EDGAR (green) and D2003 (orange). The measurements were daily-averaged and centered at 12:00 UTC. The error bars are the standard deviations of the mean values. The model results are presented as instantaneous values at 12:00 UTC.

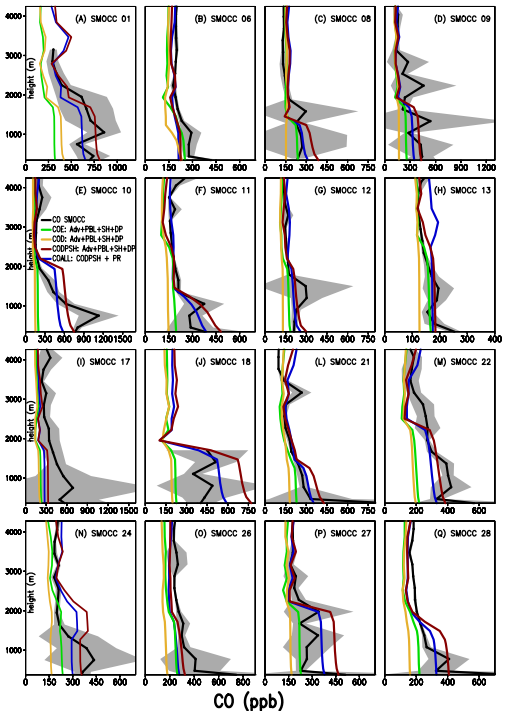

Fig. 5. Comparison between CO concentrations (ppb) observed during sixteen flights of the SMOCC/RaCCI field campaign (black solid line represents the mean while the grey zone shows the standard deviation range) and model results: using the EDGAR inventory (green), D2003 (orange), 3BEM without (red) and with (blue) plume rise.

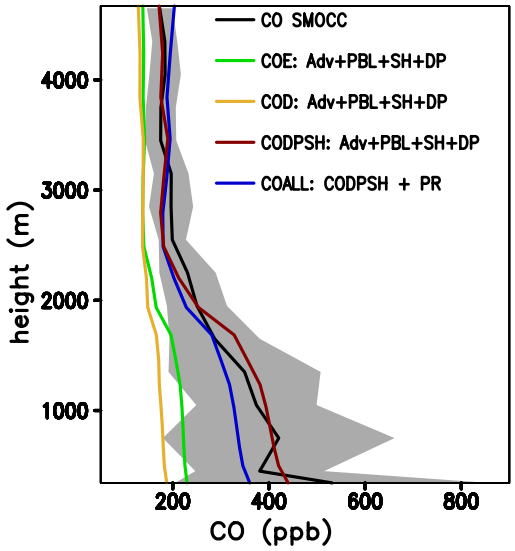

Fig. 6. Comparison between the mean CO concentrations (ppb) observed during sixteen flights of the SMOCC/RaCCI field campaign (black solid line represents the mean while the grey zone shows the standard deviation range) and the mean of model results: following the EDGAR inventory (green), D2003 (orange), 3BEM without (red) and with (blue) the plume rise mechanism.

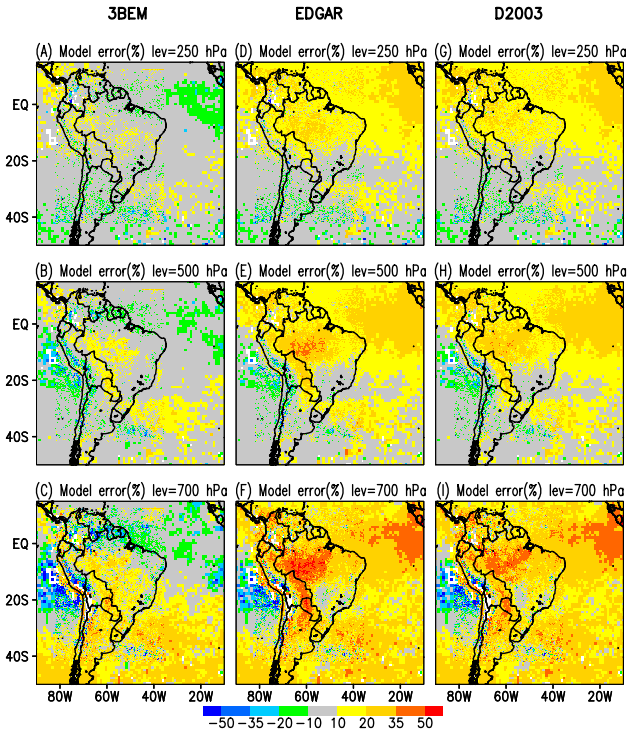

Fig. 7. CO model relative error (%) associated with the inventories 3BEM (left), EDGAR (center) and D2003 (right) in reference to the MOPITT CO retrieval for August 2002 at 3 vertical levels (700, 500 and 250 hPa). Positive values mean that model results are underestimated in reference to the MOPITT retrieved data and vice-versa.

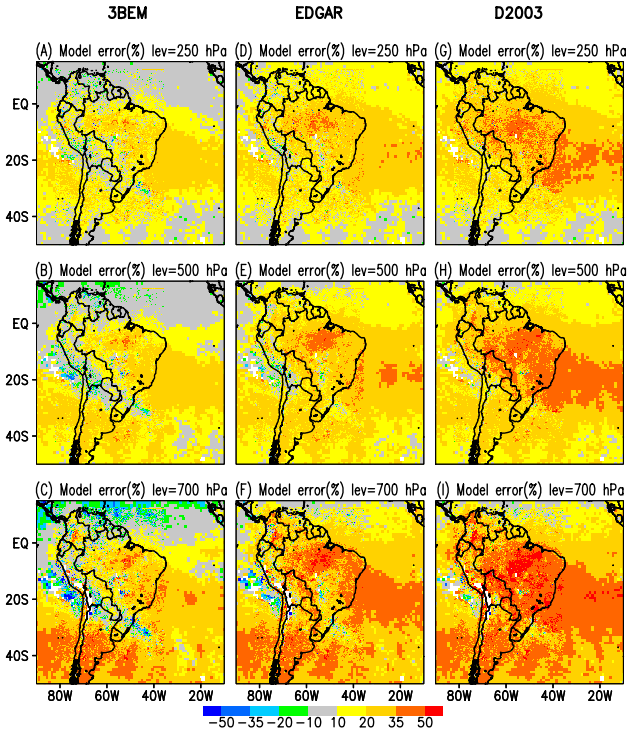

Fig. 8. CO model relative error (%) associated with the inventories 3BEM (left), EDGAR (center) and D2003 (right) in reference to the MOPITT CO retrieval for October 2002 at 3 vertical levels (700, 500 and 250 hPa). Positive values mean that model results are underestimated in reference to the MOPITT retrieved data and vice-versa.